Significant increase of Curie temperature in nano-scale BaTiO3

Yueliang Li, Zhenyu Liao, Fang Fang, Xiaohui Wang, Longtu Li, and Jing Zhu

Articles you may be interested in

Structural and dielectric properties of laser ablated BaTiO3 films deposited over electrophoretically dispersed CoFe2O4 grains
J. Appl. Phys. **116**, 164112 (2014); 10.1063/1.4900516

Multiferroic Ni0.6Zn0.4Fe2O4-BaTiO3 nanostructures: Magnetoelectric coupling, dielectric, and fluorescence
J. Appl. Phys. **116**, 124103 (2014); 10.1063/1.4896118

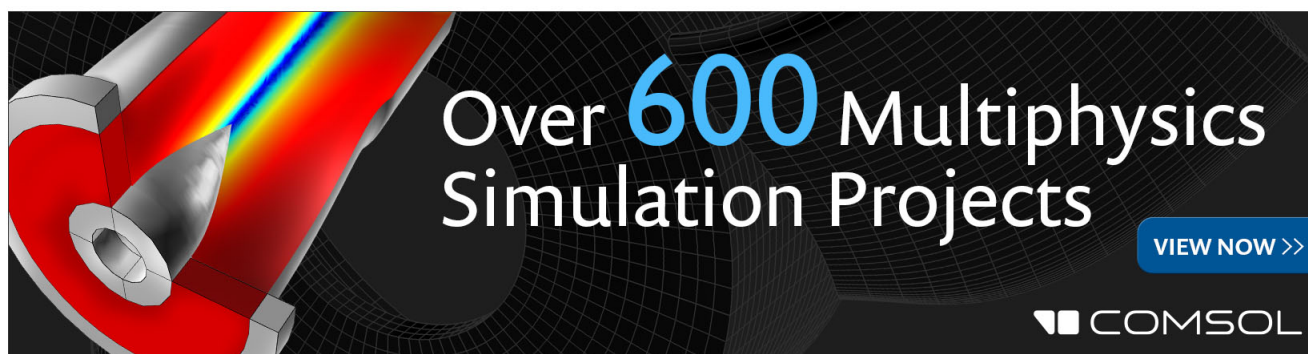Structure, piezoelectric, and ferroelectric properties of BaZrO3 substituted Bi(Mg1/2Ti1/2)O3-PbTiO3 perovskite
J. Appl. Phys. **111**, 104118 (2012); 10.1063/1.4722286

Raman spectroscopic study of Na1/2Bi1/2TiO3-x%BaTiO3 single crystals as a function of temperature and composition
J. Appl. Phys. **109**, 113507 (2011); 10.1063/1.3587236

Dielectric behavior of Fe-ion-doped BaTi O 3 nanoparticles
J. Appl. Phys. **97**, 044311 (2005); 10.1063/1.1846135

Significant increase of Curie temperature in nano-scale BaTiO₃

Yueliang Li,[1] Zhenyu Liao,[1] Fang Fang,[1] Xiaohui Wang,[2] Longtu Li,[2] and Jing Zhu[1,a)]
[1]*National Center for Electron Microscopy in Beijing, School of Materials Science and Engineering, State Key Laboratory of New Ceramics and Fine Processing, Laboratory of Advanced Materials (MOE), Tsinghua University, Beijing 100084, China*
[2]*State Key Laboratory of New Ceramics and Fine Processing, School of Materials Science and Engineering, Tsinghua University, Beijing 100084, China*

The low Curie temperature ($T_c = 130\,°C$) of bulk BaTiO₃ greatly limits its applications. In this work, the phase structures of BaTiO₃ nanoparticles with sizes ranging from 2.5 nm to 10 nm were studied at various temperatures by using aberration-corrected transmission electron microscopy (TEM) equipped with an *in-situ* heating holder. The results implied that each BaTiO₃ nanoparticle was composed of different phases, and the ferroelectric ones were observed in the shells due to the complicated surface structure. The ferroelectric phases in BaTiO₃ nanoparticles remained at 600 °C, suggesting a significant increase of T_c. Based on the *in-situ* TEM results and the data reported by others, temperature-size phase diagrams for BaTiO₃ particles and ceramics were proposed, showing that the phase transition became diffused and the T_c obviously increased with decreasing size. The present work sheds light on the design and fabrication of advanced devices for high temperature applications. © 2014 Author(s). All article content, except where otherwise noted, is licensed under a Creative Commons Attribution 3.0 Unported License.
[http://dx.doi.org/10.1063/1.4901169]

Ferroelectric, as one of the most important functional materials, has played an irreplaceable role for the rapid development of modern electronic industry in the past few decades.[1] It is the key raw material for production of capacitors with ultra-high capacitance for its extremely high dielectric constant,[2] and also used in memory devices with wide applications.[3–5] Moreover, ferroelectrics have great potential in various fields such as microelectronics,[6] integrated optics,[7] and optoelectronics.[8]

BaTiO₃ is one of the most typical lead-free ferroelectrics with perovskite structures. It is not only widely used as a conventional ferroelectric but also recently introduced in components of multi-layer ceramic capacitors[9] and multiferroics.[10] Nevertheless, the use of bulk BaTiO₃ is limited due to its low Curie temperature ($T_c = 130\,°C$ (Ref. 11)). It motivates interests in increasing the T_c to extend the applications of ferroelectrics to higher temperatures.

It is well known that ferroelectricity is associated with a variety of phases and is temperature-dependent for bulk BaTiO₃. At high temperature, the paraelectric cubic (C) phase shows no ferroelectricity. It transforms to the tetragonal (T) phase, the orthorhombic (O) phase, and the rhombohedral (R) phase, which are all ferroelectric, when the temperature decreases to 130 °C (T_c), 5 °C, and −75 °C, respectively.[11]

Reducing the size from bulk to nanoscale significantly effects the physical and chemical properties of functional and structural materials and thus their applications.[12,13] The size effect in BaTiO₃ has been intensively studied. Anliker *et al.*[14] investigated the properties of very fine (several micrometers) BaTiO₃ particles by employing x-ray diffraction, electron diffraction, and dielectric measurement techniques, and found that the cubic-tetragonal transition became smeared out with decreasing particle size. Thanks to the development of nanotechnology, particles with size down to 5 nm were prepared.[15] Multi-phase coexistence was then found in BaTiO₃ nanoparticles in the range from 5 nm to 100 nm by using high resolution synchrotron x-ray diffraction.[16] The same phenomenon was further confirmed by Han in 2013 (Ref. 17) and Sendova in 2014.[18] They found that the ferroelectric phase did not disappear but became diverse and complicated as the particle size decreased.

Research on the grain size effect in BaTiO₃ ceramic also has a long history. Herczog[19] found that the dielectric constant of polycrystalline BaTiO₃ at room temperature increased toward the peak value at a grain size of 1 μm, and decreased with decreasing grain size in the range from 1 to 0.1 μm. In 1967, Miller[20] measured the dielectric constant of BaTiO₃ at different temperatures with grain sizes of 60 μm, 35 μm, 25 μm and 18 μm; the dielectric constant decreased with decreasing grain size, while the location of peaks in the dielectric-temperature spectrum did not shift with different grain sizes. Kinoshita *et al.*[21] found that the dielectric constant in high-purity BaTiO₃ ceramics depended on the grain size in the ferroelectric phase, while no dependence was found in the paraelectric phase. The peaks at the T-O and O-R phase transition temperatures in the dielectric-temperature spectrum seemed to shift to higher temperature with decreasing grain size, while no shift was found at the C-T transition point. Arlt *et al.*[22] studied the dielectric properties and structures of BaTiO₃ ceramic with grain size from 0.3 to 100 μm. They observed a higher dielectric constant in fine-grained BaTiO₃, and a phase transition from tetragonal to pseudocubic with grain sizes smaller than 1 μm at room temperature. They also discovered an increase in the T-O transition temperature at a grain size of 0.7 μm. In 1993, Fang *et al.*[23] achieved the maximal dielectric constant of 6100 at grain size of 1.2 μm in BaTiO₃. BaTiO₃ ceramics with grain size of nanometers were prepared before 2005 by Zhao[24] and

---

a)Author to whom correspondence should be addressed. Electronic mail: jzhu@mail.tsinghua.edu.cn
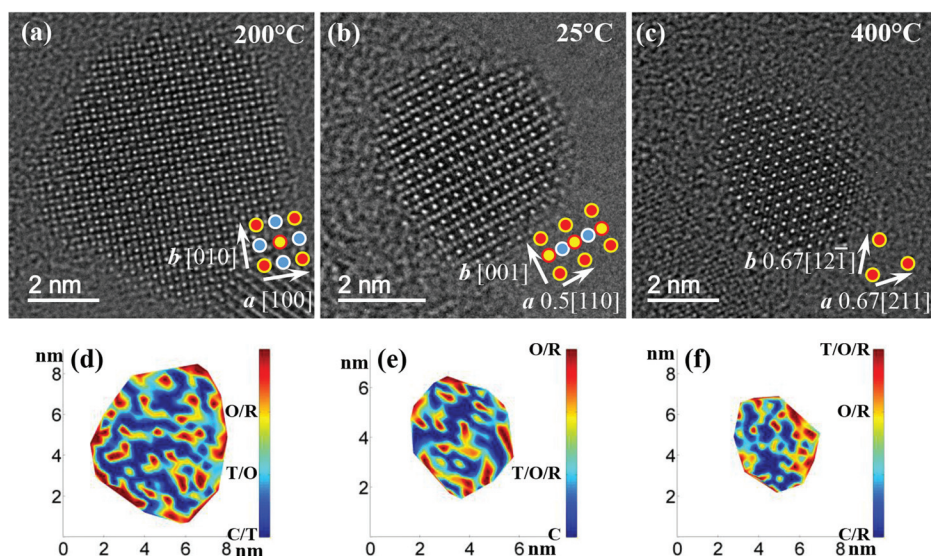
105, 182901-1

FIG. 1. (a)–(c) Atomic resolved TEM images of $BaTiO_3$ nanoparticles with the incident electron beam parallel to $\langle 100 \rangle$, $\langle 110 \rangle$, and $\langle 111 \rangle$, recorded at 200 °C, 25 °C, and 400 °C, respectively. (d)–(f) The distribution mappings of possible phases related with the corresponding symmetry, where phase with high symmetry locates in cool areas and low symmetric phases locate in warm areas.

Buscaglia[25] by employing spark plasma sintering. They found that phase transitions became more diffuse with decreasing grain size in nano-grained $BaTiO_3$ ceramics, implying possible phase-coexistence. Zhao *et al.* also predicted that the nano-grained $BaTiO_3$ ceramic would lose ferroelectricity below a critical grain size of 10 to 30 nm. In 2006, the minimal grain size was reduced again. Wang *et al.*[26] obtained $BaTiO_3$ ceramic with a grain size of only 8 nm using a two-step sintering method. The grain size was further reduced to 5 nm in 2011.[15] Raman spectra and dielectric investigations showed the coexistence of various phases, suggesting that ferroelectricity remains in $BaTiO_3$ ceramics with grain size as small as only a few nanometers.[27]

The reported works show that size has significant influences on phase structure, phase transition temperature including T_c, and thus on dielectric and ferroelectric properties for $BaTiO_3$. However, due to the limitations in probing techniques and variations of samples size, the acquired experimental data is averaged due to the poor spatial resolutions of the probing instruments. Therefore, studies on phase structure of a single particle (or grain) and exploring the origin of the size effect on T_c is highly needed. Resolution of transmission electron microscope (TEM) has been greatly improved due to the invention of the aberration-corrector.[28] The negative Cs

imaging (NCSI) technique allows atoms to appear bright on a dark background.[29] Combing aberration-corrected TEM with the NCSI technique, positions of each atom can be accurately measured for more detailed analysis,[30–33] making the determination of phase structure possible. Moreover, exploration of the phase structure at various temperatures is also possible with an *in-situ* heating holder. In this work, we used the NCSI technique and an *in-situ* heating holder to understand the nature of size effect on T_c in $BaTiO_3$, and proposed experimentally derived size-temperature phase diagrams.

$BaTiO_3$ nanoparticles with an average size of 5 nm were synthesized by one-step solvothermal method.[15] The nanoparticles were then dispersed on the DENSsolutions' consumable EMheaterchipTM[34] for subsequent *in-situ* TEM observation. In our experiment, the EMheaterchipTM was heated up to 600 °C inside the DENSsolutions single tilt holder by the sample heating system. An FEI Titan 80–300 aberration-corrected TEM was used to record atomically resolved images at various temperatures under the NCSI condition with Cs = −13 µm and an overfocus of 6 nm. The position of each atomic column was accurately measured by fitting two-dimensional Gaussian functions to areas close to their intensity maxima.

Figs. 1(a)–1(c) show the atomically resolved TEM images of $BaTiO_3$ nanoparticles with the incident electron
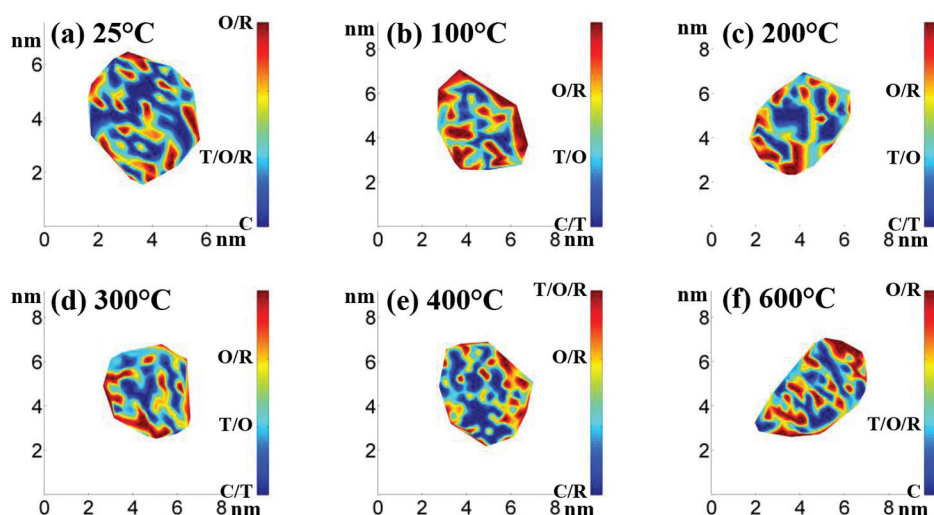

FIG. 2. Phase distribution maps of six different particles with the similar size (4-5 nm) at (a) 25 °C, (b) 100 °C, (c) 200 °C, (d) 300 °C, (e) 400 °C, and (f) 600 °C, respectively. All the particles are composed of various phases including ferroelectric phases with lower symmetry, implying that ferroelectric phases could remain at 600 °C and the T_c increases to at least 600 °C in $BaTiO_3$ nanoparticle.
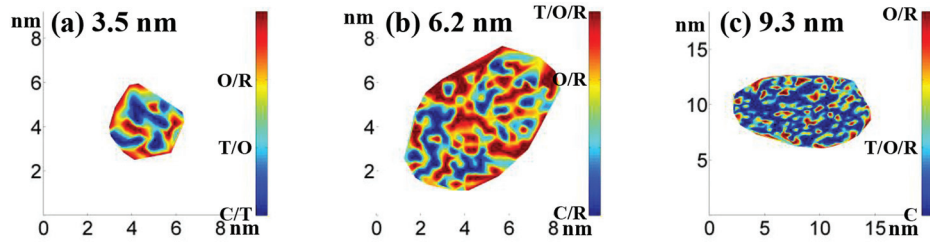
FIG. 3. Phase distribution maps of three different particles with the size of (a) 3.5 nm, (b) 6.2 nm, and (c) 9.3 nm at the same temperature (400 °C). Phases with lower symmetry (ferroelectric phases) are more found in the shell of the particles due to surface relaxations. The proportion of the relaxed surface significantly increases as the particle size decreases. Surface relaxation is the origin of the coexistence of various phases.

beam parallel to ⟨100⟩, ⟨110⟩, and ⟨111⟩, recorded at 200 °C, 25 °C, and 400 °C, respectively. As the coordinate of each atomic column was accurately measured, the two basis vectors ($\vec{a}$ and $\vec{b}$, denoted in Figs. 1(a)–1(c)) and angle ⟨$\vec{a},\vec{b}$⟩ of each unit cell can be obtained. The D-value between the lengths of the two basis vectors ($||\vec{a}|-|\vec{b}||$ for ⟨100⟩ and ⟨111⟩ zone axis, while $|\sqrt{2}|\vec{a}|-|\vec{b}||$ for ⟨110⟩ zone axis) and the D-value between the angles of ⟨$\vec{a},\vec{b}$⟩ and 90° (60° for ⟨111⟩ zone axis) were calculated for each unit cell in each observed particle, maps of which were drawn out, respectively.[36] Combined with the two D-value maps, symmetry transformation of each area in the observed single particle can be identified and then the distribution maps of possible phases related with the corresponding symmetry are drawn out,[36] as shown in Figs. 1(d)–1(f), where the phase with high symmetry located in cool areas while the low symmetric phases located in warm areas.

The phase distribution maps of six different particles with similar sizes (4–5 nm) at different temperatures of (a) 25 °C, (b) 100 °C, (c) 200 °C, (d) 300 °C, (e) 400 °C, and (f) 600 °C are presented in Fig. 2. The particles are all composed of various phases including ferroelectric phases with lower symmetry. Fig. 3 shows the phase distribution maps of three particles with the size of (a) 3.5 nm, (b) 6.2 nm, and (c) 9.3 nm at the same temperature (400 °C). As can be seen from Figs. 1(d)–1(f), 2, and 3, the particles with size ranging from 2.5 nm to 10 nm are all composed of various phases at 25–600 °C. No single phase-composed particle is found. We also find that warm areas prefer to exist at the outer shell of the particles, while cool areas are found mainly in the particle's core.

Each BaTiO$_3$ nanoparticle is surrounded by several different surfaces with complicated structures. Atomic shifts induced by surface relaxation will reduce the symmetry of the shell structure of the nanoparticle. The thickness of the relaxed shell is about 1 nm, accounting for a sharp increasing share of the particle as the particle size decreases to only several nanometers. Surface relaxation is the origin of the coexistence of various phases in BaTiO$_3$ nanoparticles. The multi-phase coexistence is found in BaTiO$_3$ nanoparticles at the temperature range of 25 °C to 600 °C, implying that ferroelectric phases can remain at 600 °C and the T_c significantly increases from 130 °C to at least 600 °C.

Temperature-size phase diagrams were proposed to reveal the dual effect of size and temperature in BaTiO$_3$. In the phase diagrams, the point on the phase boundary indicates the phase transition temperature with a given size, and

the critical size of phase transition at a given temperature as well. Fig. 4(a) shows the temperature-particle size phase diagram for BaTiO$_3$ particles. Particles larger than 1 μm are treated as bulk BaTiO$_3$, and have the normal phase structures as shown in the right half part of the phase diagram. The results of high resolution synchrotron x-ray diffraction[15,16] are summarized in the left half part of the diagram, according to which we draw the phase boundaries. As shown in
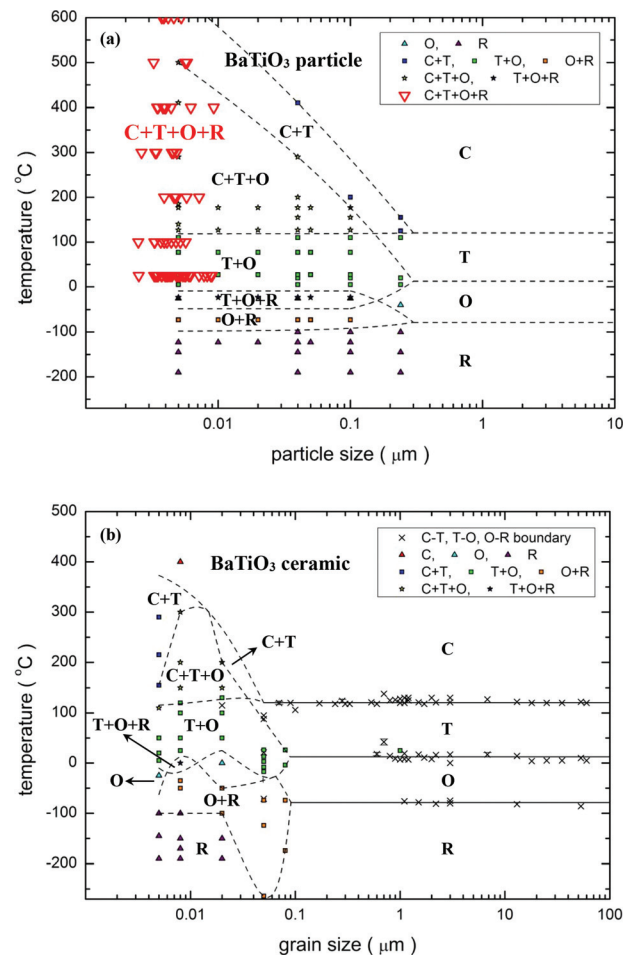

FIG. 4. Our originally created temperature-particle size phase diagram for BaTiO$_3$ particle (a) and temperature-grain size phase diagram for BaTiO$_3$ ceramic (b). The digitized data marked as color symbols except ▽ are collected from the published literatures,[15,16,20–27,35] the larger size particle (or grain) is treated as bulk BaTiO$_3$, and the corresponding area in these two phase diagrams shows the phase structure of bulk BaTiO$_3$, respectively. The data marked as red symbols ▽ are provided by this work. The phase diagrams clearly show various behaviors (e.g., T_c, the uppermost phase boundary) of BaTiO$_3$ at various size scale.

Fig. 4(a), our experimental data have been filled into the temperature-particle size phase diagram with red markers ∇. All the experimental particles are composed of C, T, O, and R phases.

Similarly, the temperature-grain size phase diagram for BaTiO$_3$ ceramics was drawn as shown in Fig. 4(b). For BaTiO$_3$ ceramics with large grain sizes (>0.1 μm), the phase boundaries are determined by the locations of peaks in the dielectric-temperature spectrums.[20–25,35] At the nanoscale, the phase structures of BaTiO$_3$ ceramics with different grain sizes are summarized in the left half part of the BaTiO$_3$ ceramics phase diagram.[15,26,27]

As shown in these two phase diagrams, nanoparticle or nano-grained BaTiO$_3$ ceramic is composed of multiple phases. As the size decreases to nanoscale, BaTiO$_3$ transforms from single phase to multi coexistent phases, that is, phase transitions become diffused and the temperature range in which ferroelectric phases remain greatly expands. The uppermost phase boundary rises in the phase diagrams as the size decreases, indicating a significant increase of T_c at the nanoscale.

In summary, multi-phase (C, T, O and R phases) coexistence in a single BaTiO$_3$ nanoparticle was revealed by employing aberration-corrected TEM equipped with an *in-situ* heating holder. Surface relaxation allows the coexistence of various phases. Based on the reported data and the present results, temperature-size phase diagrams were drawn to understand the dual effects of size and temperature for BaTiO$_3$. It is shown that BaTiO$_3$ transforms from single phase to multi coexistent phases and the T_c increases significantly as the size decreases from bulk to nanoscale. The results pave a way to realize the device applications at high temperature.

[1]W. Wu, C. Pan, Y. Zhang, X. Wen, and Z. L. Wang, Nano Today **8**, 619 (2013).

[2]G. L. Brennecka, J. F. Ihlefeld, J.-P. Maria, B. A. Tuttle, and P. G. Clem, J. Am. Ceram. Soc. **93**, 3935 (2010).

[3]S. Boyn, S. Girod, V. Garcia, S. Fusil, S. Xavier, C. Deranlot, H. Yamada, C. Carrétéro, E. Jacquet, M. Bibes, A. Barthélémy, and J. Grollier, Appl. Phys. Lett. **104**, 052909 (2014).

[4]A. M. W. Tam, G. Qi, A. K. Srivastava, X. Q. Wang, F. Fan, V. G. Chigrinov, and H. S. Kwok, Appl. Opt. **53**, 3787 (2014).

[5]Z. M. A. Lum, X. Liang, Y. Pan, R. Zheng, and X. Xu, Opt. Eng. **52**, 015802 (2013).

[6]C.-H. Lee, N. D. Orloff, T. Birol, Y. Zhu, V. Goian, E. Rocas, R. Haislmaier, E. Vlahos, J. A. Mundy, L. F. Kourkoutis, Y. Nie, M. D. Biegalski, J. Zhang, M. Bernhagen, N. A. Benedek, Y. Kim, J. D. Brock, R. Uecker, X. X. Xi, V. Gopalan, D. Nuzhnyy, S. Kamba, D. A. Muller, I. Takeuchi, J. C. Booth, C. J. Fennie, and D. G. Schlom, Nature **502**, 532 (2013).

[7]C. Xiong, W. H. P. Pernice, J. H. Ngai, J. W. Reiner, D. Kumah, F. J. Walker, C. H. Ahn, and H. X. Tang, Nano Lett. **14**, 1419 (2014).

[8]J. Shi, M. B. Starr, and X. Wang, Adv. Mater. **24**, 4683 (2012).

[9]C. Pithan, D. Hennings, and R. Waser, Int. J. Appl. Ceram. Technol. **2**, 1 (2005).

[10]H. Zheng, J. Wang, S. E. Lofland, Z. Ma, L. Mohaddes-Ardabili, T. Zhao, L. Salamanca-Riba, S. R. Shinde, S. B. Ogale, F. Bai, D. Viehland, Y. Jia, D. G. Schlom, M. Wuttig, A. Roytburd, and R. Ramesh, Science **303**, 661 (2004).

[11]X. Deng, X. Wang, H. Wen, A. Kang, Z. Gui, and L. Li, J. Am. Ceram. Soc. **89**, 1059 (2006).

[12]M. Takagi, J. Phys. Soc. Japan **9**, 359 (1954).

[13]M.-R. He, P. Xiao, J. Zhao, S. Dai, F. Ke, and J. Zhu, J. Appl. Phys. **109**, 123504 (2011).

[14]M. Anliker, H. R. Brugger, and W. Känzig, Helv. Phys. Acta **27**, 99 (1954).

[15]H. Zhang, X. Wang, Z. Tian, C. Zhong, Y. Zhang, C. Sun, and L. Li, J. Am. Ceram. Soc. **94**, 3220 (2011).

[16]J. Zhu, W. Han, H. Zhang, Z. Yuan, X. Wang, L. Li, and C. Jin, J. Appl. Phys. **112**, 064110 (2012).

[17]W. Han, J. Zhu, S. Zhang, H. Zhang, X. Wang, Q. Wang, C. Gao, and C. Jin, J. Appl. Phys. **113**, 193513 (2013).

[18]M. Sendova and B. D. Hosterman, J. Appl. Phys. **115**, 214104 (2014).

[19]A. Herczog, J. Am. Ceram. Soc. **47**, 107 (1964).

[20]C. A. Miller, Br. J. Appl. Phys. **18**, 1689 (1967).

[21]K. Kinoshita, J. Appl. Phys. **47**, 371 (1976).

[22]G. Arlt, D. Hennings, and G. de With, J. Appl. Phys. **58**, 1619 (1985).

[23]T.-T. Fang, H.-L. Hsieh, and F.-S. Shiau, J. Am. Ceram. Soc. **76**, 1205 (1993).

[24]Z. Zhao, V. Buscaglia, M. Viviani, M. Buscaglia, L. Mitoseriu, A. Testino, M. Nygren, M. Johnsson, and P. Nanni, Phys. Rev. B **70**, 024107 (2004).

[25]V. Buscaglia, M. T. Buscaglia, M. Viviani, T. Ostapchuk, I. Gregora, J. Petzelt, L. Mitoseriu, P. Nanni, a. Testino, R. Calderone, C. Harnagea, Z. Zhao, and M. Nygren, J. Eur. Ceram. Soc. **25**, 3059 (2005).

[26]X.-H. Wang, X.-Y. Deng, H.-L. Bai, H. Zhou, W.-G. Qu, L.-T. Li, and I.-W. Chen, J. Am. Ceram. Soc. **89**, 438 (2006).

[27]X. Wang, X. Deng, H. Wen, and L. Li, Appl. Phys. Lett. **89**, 162902 (2006).

[28]M. Haider, S. Uhlemann, E. Schwan, H. Rose, B. Kabius, and K. Urban, Nature **392**, 768 (1998).

[29]C. L. Jia, M. Lentzen, and K. Urban, Science **299**, 870 (2003).

[30]R. Yu, L. H. Hu, Z. Y. Cheng, Y. D. Li, H. Q. Ye, and J. Zhu, Phys. Rev. Lett. **105**, 226101 (2010).

[31]M.-R. He, R. Yu, and J. Zhu, Nano Lett. **12**, 704 (2012).

[32]M.-R. He, R. Yu, and J. Zhu, Angew. Chem. Int. Ed. Engl. **51**, 7744 (2012).

[33]L. Xie, Y. L. Li, R. Yu, Z. Y. Cheng, X. Y. Wei, X. Yao, C. L. Jia, K. Urban, A. A. Bokov, Z.-G. Ye, and J. Zhu, Phys. Rev. B **85**, 014118 (2012).

[34]J. F. Creemer, D. Briand, H. W. Zandbergen, W. van der Vlist, C. R. de Boer, N. F. de Rooij, and P. M. Sarro, Sens. Actuators, A **148**, 416 (2008).

[35]M. H. Frey, Z. Xu, P. Han, and D. A. Payne, Ferroelectrics **206**, 337 (1998).

[36]See supplementary material at http://dx.doi.org/10.1063/1.4901169 for details on the phase determination.